Original Article

Superiority of spleen stiffness on two-dimensional magnetic resonance elastography over liver stiffness and serum tests in assessing portal hypertension in chronic liver disease

Xinjun Han[1#], Dawei Yang[1#], Hui Xu[1], Yu Wang[2,3*], Hongxia Yin[1], Zhenghan Yang[1*^]

[1]Department of Radiology, Beijing Friendship Hospital, Capital Medical University, Beijing, China; [2]Liver Research Center, Beijing Friendship Hospital, Capital Medical University, Beijing, China; [3]State Key Lab of Digestive Health & National Clinical Research Center for Digestive Diseases, Beijing, China

Contributions: (I) Conception and design: Z Yang, Y Wang; (II) Administrative support: Z Yang, Y Wang, H Yin; (III) Provision of study materials or patients: Y Wang; (IV) Collection and assembly of data: X Han, D Yang; (V) Data analysis and interpretation: X Han, D Yang, H Xu; (VI) Manuscript writing: All authors; (VII) Final approval of manuscript: All authors.

[#]These authors contributed equally to this work as co-first authors.

[*]These authors contributed equally to this work as co-corresponding authors.

Correspondence to: Zhenghan Yang, MD, PhD. Department of Radiology, Beijing Friendship Hospital, Capital Medical University, 95 Yong'an Road, West District, Beijing 100050, China. Email: yangzhenghan@vip.163.com; Yu Wang, MD. Liver Research Center, Beijing Friendship Hospital, Capital Medical University, 95 Yong'an Road, West District, Beijing 100050, China; State Key Lab of Digestive Health & National Clinical Research Center for Digestive Diseases, Beijing, China. Email: wangyuliver@ccmu.edu.cn.

Background: The value of magnetic resonance elastography (MRE) in portal hypertension (PH) has yet to be determined in the context of chronic liver disease (CLD). This study examined the value of MRE for the prediction of hepatic venous pressure gradient (HVPG) and high-risk esophageal varices (EVs) in a CLD cohort with a generally high HVPG.

Methods: Patients with CLD who underwent both HVPG measurement and two-dimensional MRE examination at Beijing Friendship Hospital between April 2018 and March 2022 were prospectively included. Two-dimensional MRE was performed within the liver and spleen. Endoscopy results and laboratory parameters were collected. Some selected published serum markers were calculated, including fibrosis 4, aspartate aminotransferase-to-platelet ratio index, and King's score. The efficacy of the parameters for assessing PH was analyzed by using the Pearson correlation coefficient, linear and logistic regression, and receiver operating characteristic curve analyses.

Results: A total of 48 patients were included. The mean HVPG was 16.8±5.8 mmHg. Among these patients, 47 patients had PH (HVPG >5 mmHg), and 43 patients had clinically significant PH (HVPG ≥10 mmHg). Among the parameters associated with HVPG, the strongest correlation was found for spleen stiffness (SS) (R=0.638; P<0.001). In multiple regression analyses, SS was independently associated with an elevated HVPG and high-risk EVs. The areas under the receiver operating characteristic curve of SS for identifying patients with an HVPG ≥16 mmHg, HVPG ≥20 mmHg, and high-risk EVs were 0.790, 0.822, and 0.886, respectively, which were higher than those of liver stiffness (LS) and serum markers but slightly inferior to that of fibrosis 4 (area under the receiver operating characteristic curve =0.844) in identifying an HVPG ≥16 mmHg. SS cutoff values of 9.5, 10.05, and 9.9 kPa were selected to rule out the presence

^ ORCID: 0000-0002-8473-3257.

of an HVPG ≥16 mmHg, HVPG ≥20 mmHg, and high-risk EVs (sensitivity: 100%, 100%, and 100%, respectively; specificity: 45.5%, 50%, and 60%, respectively).

Conclusions: In patients with generally high HVPG, SS measured by two-dimensional MRE may be a better predictor of HVPG values and high-risk EVs than LS and serum markers.

Keywords: Magnetic resonance elastography (MRE); liver cirrhosis; portal hypertension (PH); esophageal varices (EV)

Submitted Dec 20, 2022. Accepted for publication Nov 17, 2023. Published online Jan 02, 2024.
doi: 10.21037/qims-22-1415
View this article at: https://dx.doi.org/10.21037/qims-22-1415

Introduction

Portal hypertension (PH) is a frequent complication of chronic liver disease (CLD) and is mainly responsible for its serious consequences, which include variceal hemorrhage, hepatic encephalopathy, and ascites (1). The accurate assessment of portal venous pressure is essential the proper treatment to reduce the mortality rate of PH-related complications (2). The current gold standard for assessing portal venous pressure remains the hepatic venous pressure gradient (HVPG) (3). However, HVPG measurement is not widely available due to its invasive nature. The risk of variceal bleeding can also be assessed via esophagogastroduodenoscopy (4), but it has similar drawbacks, including invasiveness, cost, and patient discomfort. Therefore, reliable noninvasive methods that can potentially replace HVPG measurements and endoscopy are being examined.

Over the past years, elastography has shown promising results in assessing PH, and ultrasound elastography, particularly transient elastography (TE), has been studied extensively (5). Magnetic resonance elastography (MRE) is another alternative means to measuring liver stiffness (LS) and spleen stiffness (SS). This technique is theoretically superior to ultrasound elastography since it can scan the entire liver and spleen to obtain a larger measurement area. Several preliminary studies have confirmed the value of MRE in assessing PH and esophageal varices (EVs) (6-13); however, evidence is still scarce. First, there is no clear answer as to which organ is more useful for revealing PH between the liver and the spleen. Some studies have shown that SS has significant superiority (6,7,11), while others have reported that LS is comparable or even better (10,14,15). Second, the reported cutoff values vary considerably across different studies and therefore need to be harmonized. Third, a comparison of MRE with established serum biomarkers is lacking. Fourth, the diagnostic value of MRE for higher HVPG thresholds remains unclear. Previous studies have focused mainly on the thresholds of clinically significant portal hypertension (CSPH) (HVPG ≥10 mmHg) and severe PH (HVPG ≥12 mmHg) (6,7,10,15). However, the risk stratification of patients above these thresholds remains clinically important. There is evidence that an HVPG higher than 16 and 20 mmHg is associated with poor prognosis (higher mortality with HVPG above 16 (16,17), while an HVPG above 20 is associated with a higher failure rate to control bleeding (18).

Therefore, the aim of this study was to assess the predictive power of LS and SS for HVPG and high-risk EVs in a cohort of patients with CLD and a generally high HVPG and to compare them with several established serum biomarkers. We present this article in accordance with the STROBE reporting checklist (available at https://qims.amegroups.com/article/view/10.21037/qims-22-1415/rc).

Methods

Patients

In this prospective study, patients with CLD who underwent HVPG measurement at the Department of Hepatology, Beijing Friendship Hospital, between April 2018 and March 2022 were screened for enrolment. The exclusion criteria for patients were as follows: a history of transjugular intrahepatic portosystemic shunt (TIPS), splenectomy, hepatectomy, liver transplantation or partial splenic embolization, portal system thrombosis, previous or ongoing nonselective beta-blocker (NSBB) treatment, episodes of recent variceal bleeding, hepatic venous-to-venous communications, contraindications to MRE, and refusal to participate. The diagnosis of CLD was confirmed on the basis of the results of liver histology or clinical,

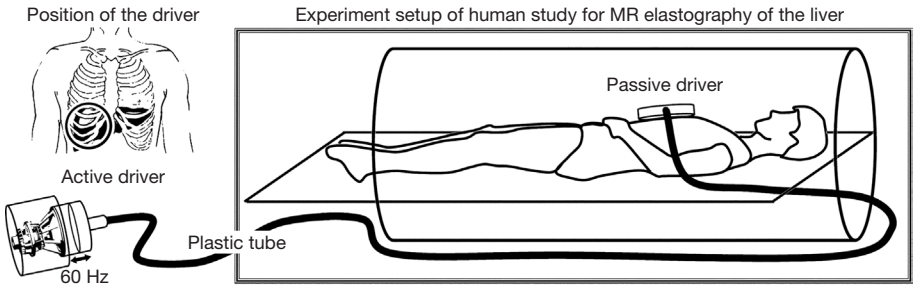

Figure 1 System for applying shear waves to the abdomen for MR elastography of the liver. Acoustic pressure waves (at 60 Hz) are generated by an active audio driver, located away from the magnetic field of the MR imaging unit, and transmitted via a flexible tube to a passive pneumatic driver placed over the anterior body wall. The diagram on the left is a coronal illustration of the location of the passive pneumatic driver (circle) with respect to the liver. This image is from Yin *et al.* (21), and the permission for its reuse was obtained. MR, magnetic resonance.

biochemical, and radiologic findings. The study was conducted in accordance with the Declaration of Helsinki (as revised in 2013) and approved by the Institutional Review Board of Beijing Friendship Hospital (no. 2018-P2-142-01). Informed consent was obtained from all patients.

HVPG measurement

All patients, after an overnight fast, underwent HVPG measurement conducted by 2 experienced hepatologists (W.Y. and H.F., with 5 and 10 years of experience with HVPG measurement, respectively). Under local anesthesia, a 6-F venous introducer was inserted into the right internal jugular vein via the Seldinger technique. Under fluoroscopic control, a balloon-tipped catheter was inserted into the right hepatic vein to measure the wedged hepatic venous pressure (WHVP) and free hepatic venous pressure (FHVP). The HVPG was recorded as the difference between the WHVP and FHVP. Permanent pressure tracings were recorded and printed. At least three valid measurements were carried out in each patient, with their average being taken as the final result.

Upper gastrointestinal endoscopy

We collected the endoscopy results of the patients who were admitted for HVPG measurement. Endoscopy was performed by experienced endoscopists. EVs were classified into four groups as follows according to international guidelines (19): (I) F0, lack a varicose appearance; (II) F1 straight, small-caliber varices; (III) F2 moderately enlarged, beady varices; and (IV) F3, markedly enlarged, nodular or tumor-shaped varices. The presence of the red color (RC) sign was also recorded. High-risk EVs were defined as F2 to F3 varices or F1 varices with RC according to the Baveno VI criteria (20).

MRE imaging and processing

Within a week before HVPG measurement (mean, 2.4 days; range, 1–6 days), MRE examinations were performed on a 3.0-T MRI machine (750 W; GE HealthCare, Chicago, IL, USA). After fasting for at least 6 hours, patients were scanned in the supine position, and an elastic band was used to secure a 19-cm-diameter passive driver against the upper abdomen (over the right upper abdomen at the level of the xiphoid process). The MRE scan was consistent with that described in Yin *et al.*'s study (21), with *Figure 1* showing the schematic. A 60-Hz vibration was generated by the active driver (Resoundant, Inc., Rochester, MN, USA) and delivered by the plastic hose connected to the passive driver, which transmitted the vibrations into the liver and spleen. MRE data were acquired using the breath-hold two-dimensional spin echo-echo planar imaging (SE-EPI) sequence. The MRE sequence parameters were as follows: axis position; repetition time/echo time (TR/TE) 1,000 ms/Min Full; matrix, 64×64; field of view (FOV), 42 cm ×42 cm; slice thickness, 10 mm; slice gap, 5 mm; number of layers, 7; excitation times, 3; bandwidth, 250 Hz; driver frequency, 60 Hz; amplitude, 70%; and time to complete the scan with three breath-holds, 51 s.

MRE data were analyzed by an experienced radiologist (with more than 5 years of experience in MRE) using the Volume Viewer postprocessing software (version 13.0, GE HealthCare) who was blinded to the HVPG and clinical

data. An inversion algorithm (22) was used to postprocess the wave information, generating wave, magnitude, and elastogram images. Regions of interest (ROIs) were drawn on the anatomical images and copied to the elastogram for reading. The ROI needed to be drawn as large as possible on the liver and spleen parenchyma, with large vessels, organ edges, and areas with crosshatch (a confidence level of less than 0.95) or with poor wave propagation in the corresponding wave images being avoided. Measurements were performed on the center three slices of the liver and spleen, and the average value of the ROI for three slice locations was used as the stiffness value.

Clinical and laboratory data collection

Demographic data, including age, sex, BMI, and cause of CLD, were collected from all patients. Additionally, laboratory parameters, including platelet (PLT) count, biochemical data, and coagulation profiles, were obtained within the week prior to MRE, upper gastrointestinal endoscopy, and HVPG. The Child-Pugh score (23) and the model for end stage liver disease (MELD) score (24) were calculated.

The following published serum biomarkers were evaluated in all patients: aspartate aminotransferase (AST)-to-PLT ratio index (APRI), fibrosis 4, and King's score (25). The formulae for each were as follows:

$$\text{fibrosis 4}=\frac{\text{age}\times\text{AST}}{\text{PLT}\times\text{ALT}^{\frac{1}{2}}} \quad [1]$$

$$\text{APRI}=\frac{\text{AST/ULN}}{\text{PLT}\left(10^{9}/\text{L}\right)}\times 100 \quad [2]$$

$$\text{King's score}=\text{Age}\times\text{AST}\times\frac{\text{INR}}{\text{PLT}} \quad [3]$$

Statistical analysis

Depending on the normality of the data, continuous variables are expressed as the mean ± standard deviation (SD) or as the median and interquartile range. Qualitative variables are expressed as absolute values and relative frequencies. The correlations between all the variables (including LS, SS, and clinical and imaging parameters) and HVPG were computed using the Pearson correlation coefficient. Factors that significantly correlated with HVPG in the univariable analyses were included in a multivariable stepwise linear regression analysis. Binary logistic regression analysis was performed to determine the factors associated with the presence of an HVPG ≥16 mmHg, HVPG ≥20 mmHg, and high-risk EVs. Variables with a P value less than 0.1 in univariable analysis were entered into multivariable forward stepwise analysis. To avoid the effect of collinearity, composite parameters, Child-Pugh score, MELD score, fibrosis 4, APRI, and King's score were not included in the multivariable model either in linear or in logistic regression analysis.

The diagnostic performance of the different noninvasive methods for HVPG ≥16 mmHg, HVPG ≥20 mmHg, and high-risk EVs was assessed via receiver operator characteristic (ROC) curves analysis. The performance was compared using the DeLong method (26). The optimal cutoff points for identifying HVPG ≥16 mmHg and ≥20 mmHg were determined using the highest Youden index. The cutoff for ruling out high-risk EVs was selected by optimizing the percentage of endoscopies spared and by keeping the risk of high-risk EVs below the 5% threshold, as recommended by the Baveno VI consensus (20). The sensitivity, specificity, positive likelihood ratio (+LR), and negative likelihood ratio (–LR) were calculated. All tests were two-sided, and the α value was set at 0.05. Data analysis was performed with SPSS software version 26.0 (IBM Corp., Armonk, NY, USA).

Results

Patient characteristics (Figure 2, Table 1)

A total of 49 patients with CLD underwent HVPG and MRE. One patient was excluded due to a failure of MRE. The process of patient enrolment is shown in *Figure 2*. The clinical, biochemical, endoscopic, and MRE characteristics of the 48 patients are presented in *Table 1*. The median age was 56.0 years, 21 (43.8%) patients were male, and the mean HVPG was 16.8±5.8 mmHg (range, 4–28 mmHg). Among the patients, 47 (97.9%) had PH, and 43 (87.8%) had CSPH. Moreover, 36 of the 48 patients underwent upper gastrointestinal endoscopy, 28 patients had EVs (77.8%), and 24 had high-risk EVs (66.7%).

Correlations between LS, SS, and HVPG (Figure 3)

There was a weak correlation between LS and HVPG (r=0.292; P=0.04), and a strong correlation between SS and HVPG (r=0.638; P<0.001). In patients with CSPH at HVPG ≥10 mmHg (n=43), SS was moderately linearly correlated with HVPG (r=0.526; P<0.001), while no correlation was found between LS and HVPG (r=0.040; P=0.80).

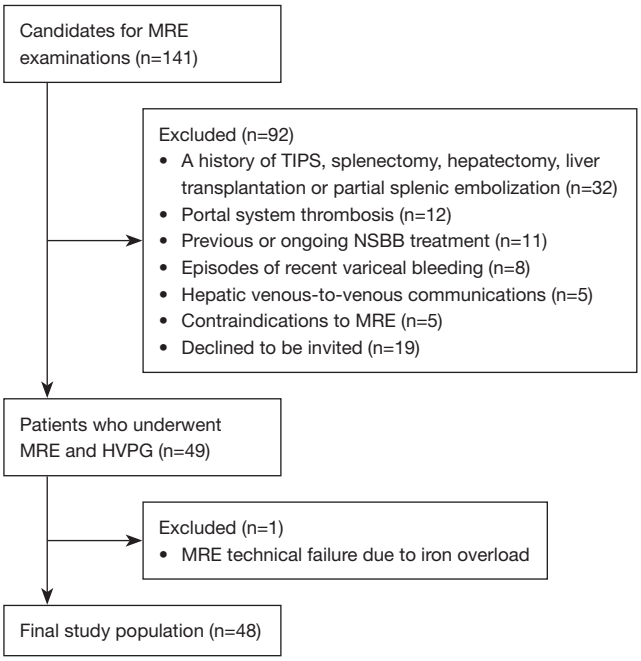

Figure 2 Flowchart showing the patient selection in this study. HVPG, hepatic venous pressure gradient; NSBB, nonselective beta-blocker; TIPS, transjugular intrahepatic portosystemic shunt; MRE, magnetic resonance elastography. NSBB, nonselective beta-blocker.

Factors associated with HVPG (Table 2)

In the univariable linear regression analysis, HVPG was significantly associated with age, PLT count, international normalized ratio (INR), MRE-LS, MRE-SS, Child-Pugh score, fibrosis 4, APRI, and King's score. Among all the parameters, MRE-SS had the highest correlation coefficient (r=0.638; P<0.001). When analyzed by multivariable linear regression, age (β coefficient =0.295; P=0.002), INR (β coefficient =0.375; P<0.001), and MRE-SS (β coefficients =0.61; P<0.001) remained independently associated with HVPG. Neither the PLT count nor MRE-LS retained statistical significance (*Table 2*).

Parameters for identifying elevated HVPG and high-risk EVs (Tables S1-S3)

PLT count, INR, MRE-SS, Child-Pugh score, and fibrosis 4 were associated with the presence of HVPG ≥16 mmHg according to univariable logistic regression analysis (P=0.01, 0.08, 0.001, 0.02, and 0.003, respectively) (Table S1). Only MRE-SS was selected as an independent factor in the

Table 1 Patient characteristics

Variable	Data
Age, years	56.0±17.0 [20–73]
Gender, M/F	21/27
BMI, kg/m^2	24.5±4.3 [16.9–36.2]
Etiology	
Hepatitis B	6 (12.2)
Alcohol	8 (16.3)
NAFLD	8 (16.3)
Autoimmune liver disease	7 (14.3)
Primary biliary cholangitis	11 (22.4)
Other	4 (8.2)
Cryptogenic	4 (8.2)
Albumin, g/L	32.4±8.8 [21.2–64.5]
Total bilirubin, μmol/L	31.9±35.3 [10.7–363.7]
AST, U/L	46.1±86.1 [18.3–547.7]
ALT, U/L	36±74 [11–377]
Prothrombin time, s	12.1±0 [11.2–17.5]
International normalized ratio	1.3±0.3 [0.88–2.07]
Platelet count, ×10^9/L	74.5±6.5 [19–303]
Serum creatinine, μmol/L	59.5±25.9 [32.6–103.2]
Child–Pugh score	7.0±3.0 [5–12]
Child–Pugh classification	
A	17 (34.7)
B	19 (38.8)
C	12 (24.5)
MELD score	9.6±4.5 [0.5–18.7]
Liver stiffness, kPa	6.7±3.3 [3.4–12.2]
Spleen stiffness, kPa	11.8±2.9 [6.1–18.2]
HVPG, mmHg	16.8±5.8 [4–28]
HVPG ≥5, mmHg	47 (97.9)
HVPG ≥10, mmHg	43 (87.8)
Underwent GI endoscopy	36 (75.0)
Presence of EVs	28 (77.8)
High-risk EVs	24 (66.7)

The total number of participants analyzed was 48. Data are expressed the mean ± standard deviation or median and IQR with range in square brackets, or numbers of patients with percentages in parentheses. IQR, interquartile range; BMI, body mass index; NAFLD, nonalcoholic fatty liver disease; AST, aspartate transaminase; ALT, alanine transaminase; MELD, model for end-stage liver disease; HVPG, hepatic venous pressure gradient; GI, gastrointestinal; EVs, esophageal varices.

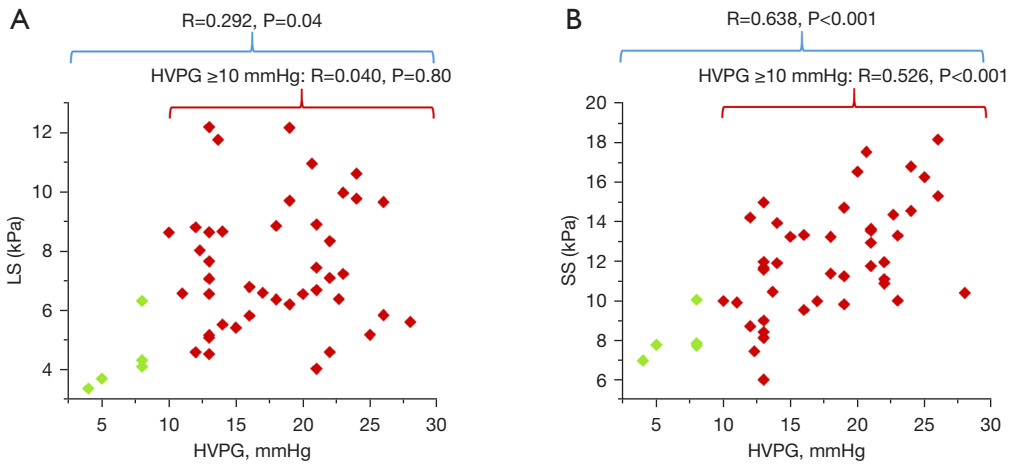

Figure 3 Correlation of HVPG with liver and spleen stiffness. (A) LS; (B) SS. HVPG, hepatic venous pressure gradient; LS, liver stiffness; SS, spleen stiffness.

Table 2 Factors associated with HVPG according to univariable and multivariable linear regression analyses

Variable	Univariable		Multivariable	
	Correlation coefficient	P	β coefficient	P
Age	0.314	0.03	0.295	0.002
BMI	−0.037	0.80		
Albumin	−0.269	0.06		
Total bilirubin	0.172	0.24		
Serum creatinine	−0.136	0.36		
AST	0.183	0.21		
ALT	−0.085	0.57		
Platelet count	−0.550	<0.001		
Prothrombin time	−0.074	0.62		
INR	0.408	0.004	0.375	<0.001
MRE-LS	0.292	0.04		
MRE-SS	0.638	<0.001	0.61	<0.001
Child-Pugh score	0.422	0.003		
MELD score	0.150	0.31		
Fibrosis 4	0.560	<0.001		
APRI	0.327	0.02		
King's score	0.363	0.01		

Bolded type indicates variables included in the multivariable analysis. BMI, body mass index; AST, aspartate transaminase; ALT, alanine transaminase; INR, international normalized ratio; MRE-LS, magnetic resonance elastography–liver stiffness; MRE-SS, magnetic resonance elastography–spleen stiffness; MELD, model for end-stage liver disease; APRI, aspartate aminotransferase-to-platelet ratio index.

Table 3 Comparison of AUCs for predicting elevated HVPG and presence of high-risk EVs

Parameter	HVPG ≥16 mmHg	HVPG ≥20 mmHg	High-risk EVs
MRE-LS	0.642 (0.490–0.775)	0.593 (0.441–0.732)	0.632 (0.455–0.786)
MRE-SS	0.790 (0.662–0.918)	0.822 (0.707–0.938)	0.886 (0.764–1.000)
Albumin	0.695 (0.543–0.846)	0.707 (0.550–0.865)	0.705 (0.522–0.887)
Total bilirubin	–	–	0.743 (0.574–0.911)
Platelet count	0.771 (0.632–0.910)	0.741 (0.594–0.888)	0.803 (0.650–0.956)
Child-Pugh score	0.708 (0.559,0.857)	–	–
MELD score	–	–	0.721 (0.550–0.892)
Fibrosis 4	0.844 (0.729–0.960)	0.778 (0.642–0.913)	–
APRI	0.745 (0.598–0.891)	0.685 (0.533–0.837)	–
King's score	0.797 (0.656–0.899)	0.743 (0.600–0.886)	–

Data are AUCs with 95% confidence intervals in parentheses. AUC, area under curve; HVPG, hepatic venous pressure gradient; EVs, esophageal varices; MRE-LS, magnetic resonance elastography–liver stiffness; MRE-SS, magnetic resonance elastography–spleen stiffness; MELD, model for end-stage liver disease; APRI, aspartate aminotransferase-to-platelet ratio index.

multivariable logistic regression analysis (odds ratio =1.614; 95% CI: 1.202–2.166; P=0.001) (Table S1).

Age, PLT count, INR, MRE-SS, Child-Pugh score, fibrosis 4, and King's score were associated with the presence of HVPG ≥20 mmHg according to the univariable logistic regression analysis (P=0.08, 0.03, 0.07, 0.001, 0.05, 0.01, and 0.10, respectively) (Table S2). MRE-SS was determined to be an independent factor associated with HVPG ≥20 mmHg after adjustment for INR and age in multivariable logistic regression analysis (P=0.002) (Table S2).

Total bilirubin, ALT, PLT count, MRE-SS, and MELD score were associated with the presence of high-risk EVs according to univariable logistic regression analysis (P=0.02, 0.09, 0.01, 0.003, and 0.04, respectively) (Table S3). Only MRE-SS was selected as an independent factor in multivariable logistic regression analysis (odds ratio =2.076; 95% CI: 1.282–3.362; P=0.003) (Table S3).

Areas under the curve (AUC) of LS, SS, and other noninvasive parameters for identifying elevated HVPG and high-risk EVs (Table 3, Tables S4-S6*)*

MRE-LS was not a significant factor in the diagnosis of HVPG ≥16 mmHg, HVPG ≥20 mmHg, or high-risk EVs, with AUCs of 0.642, 0.593, and 0.632, respectively. MRE-SS, albumin, PLT count, Child-Pugh score, fibrosis 4, APRI, and King's score were significant factors for predicting the presence of HVPG ≥16 mmHg. Among these parameters, the predictive performance of the MRE-SS (AUC =0.790; 95% CI: 0.662–0.918) was inferior to that of fibrosis 4 (AUC =0.844; 95% CI: 0.729–0.960), and King's score (AUC =0.797; 95% CI: 0.656–0.899) but superior to that of the other factors (*Table 3*).

MRE-SS, albumin, PLT count, fibrosis 4, APRI, and King's score were significant factors for predicting the presence of HVPG ≥20 mmHg. Among these parameters, MRE-SS was the most accurate predictive factor, as reflected by the highest AUC of 0.822 (*Table 3*).

For identifying high-risk EVs, MRE-SS, albumin, total bilirubin, PLT count, and MELD score were significant factors. Among these parameters, the AUC of MRE-SS (AUC =0.886; 95% CI: 0.764–1.000) was the highest. However, the difference in AUCs between each group did not reach statistical significance in the above three scenarios (Tables S4-S6).

In summary, MRE-SS had the best performance for the diagnosis of HVPG ≥20 mmHg and high-risk EVs but demonstrated no advantage over fibrosis 4 in identifying HVPG ≥16 mmHg (*Table 3*).

Diagnostic performance of LS and SS for identifying elevated HVPG and high-risk EVs (Table 4)

The MRE-SS cutoff values of 9.5 and 10.05 kPa were selected to predict the presence of HVPG ≥16 mmHg and HVPG ≥20 mmHg, respectively (HVPG ≥16 mmHg: sensitivity 100%, specificity 45.5%, +LR 1.83, –LR 0; HVPG ≥20 mmHg: sensitivity 100%, specificity 50%, +LR

Table 4 Cutoff values and diagnostic accuracies of LS and SS for the identification of elevated HVPG and high-risk EVs

Cutoff value	Sensitivity (%)	Specificity (%)	+LR	–LR
HVPG ≥16 mmHg				
SS >9.5 kPa	100	45.5	1.83	0
SS >10.6 kPa	80.8	63.6	2.22	0.3
SS >12.5 kPa	57.7	81.8	3.17	0.52
SS >14.3 kPa	34.6	95.5	7.62	0.68
LS >5.6 kPa	88.5	45.5	1.62	0.25
LS >7.1 kPa	50	63.6	1.37	0.79
LS >8.7 kPa	34.6	86.4	2.54	0.76
HVPG ≥20 mmHg				
SS >10.05 kPa	100	50	2	0
SS >11.0 kPa	83.3	56.7	1.92	0.29
SS >13.5 kPa	55.6	86.7	4.17	0.51
SS >14.3 kPa	44.4	93.3	6.67	0.6
LS >5.6 kPa	83.3	33.3	1.25	0.5
LS >6.7 kPa	61.1	56.7	1.41	0.69
LS >8.9 kPa	33.3	86.7	2.50	0.77
High-risk EVs				
SS >9.9 kPa	100	60	2.5	0
SS >10.6 kPa	90.5	80	4.52	0.12
SS >11.5 kPa	81.0	86.7	6.07	0.22
SS >13.3 kPa	57.1	93.3	8.57	0.46
SS >14.3 kPa	33.3	93.3	5	0.71
LS ≤5.6 kPa	33.3	80	1.67	0.83
LS ≤6.3 kPa	47.6	73.3	1.79	0.71
LS ≤6.8 kPa	76.2	66.7	2.29	0.36
LS ≤7.5 kPa	85.7	53.3	1.84	0.27

LS, liver stiffness; SS, spleen stiffness; HVPG, hepatic venous pressure gradient; EVs, esophageal varices; +LR, positive result likelihood ratio; –LR, negative likelihood ratio.

2, –LR 0) (*Table 4*).

The cutoff value of MRE-SS was set to 9.9 kPa to rule out high-risk EVs, which could spare 9 of 15 (60%) patients from unnecessary endoscopy, with a 0% risk of missing high-risk EVs (0/21). The sensitivity for the identification of patients with high-risk EVs was 100%, the specificity was 60%, the +LR was 2.5, and the –LR was 0. *Table 4* shows the diagnostic ability of LS and SS at different thresholds.

Discussion

The main findings of this study can be summarized as follows: (I) SS measured by two-dimensional MRE has a closer linear relationship with HVPG than does LS and routinely used serum tests. (II) SS demonstrated the best performance in predicting HVPG ≥20 mmHg and high-risk EV but was less accurate than was fibrosis 4 in detecting HVPG ≥16 mmHg. (III) We recommend that despite its low specificity, SS be used to rule out the use of the proposed thresholds owing to its excellent sensitivity.

Literature on MRE in PH using HVPG as a reference standard are scarce. We found a total of six studies with human participants, five of which assessed both the liver and spleen (6,7,10,11,15) and one of which assessed only LS (14). The correlation coefficient of hepatic viscoelastic parameters with HVPG reported in these studies ranged from 0.407 to 0.92, which was higher than the result of our study (r=0.292). We attribute this discrepancy to the study population, which in our study consisted mainly of patients with advanced PH, who typically have higher HVPG values. It is believed that the correlation of LS and HVPG decreases significantly in the higher HVPG range (27-29). Our data support and add to the evidence that LS is not a valuable indicator of HVPG in advanced PH.

In our series of patients with HVPG measurements, we found that the stiffness of the spleen is better at predicting PH severity than is the liver. These results are in line with published data regarding ultrasound and MRE methods (6,7,11,15,30,31). The superior performance of SS over LS may be related to the pathophysiological changes in the development of PH. As liver fibrosis progresses in CLD, the subsequent morphological changes cause elevated intrahepatic resistance and concomitant portal pressure increase (32). However, as PH progresses, extrahepatic factors such as hyperdynamic circulation begin to play a role in maintaining elevated portal pressure (33). Increased SS is produced by temporary upturns in hydrostatic pressure, stemming from tissue congestion, whereas LS reflects both the variations of PH-induced congestion and liver fibrosis (34). This may partly explain why SS is more directly linked to HVPG. However, this finding was not consistently described across other studies. In the study of Wagner *et al.* (10), no significant correlation was observed between HVPG and SS with MRE. It is reasonable to suspect that the diagnostic ability of liver and

SS for PH is strongly influenced by the characteristics of the patient population, such as etiology, stage of disease, and distribution of HVPG. More studies are needed to determine their respective values in different clinical settings.

Identification of the progression of PH beyond the threshold of CSPH has gained considerable attention in recent years. However, evidence for a higher HVPG thresholds is scarce. We believe this is also clinically important because HVPG increases on a continuous scale and retains prognostic value for further decompensation and patient survival even if it exceeds the threshold of CSPH (35). Only two studies have reported the noninvasive prediction of HVPG at higher cutoff values. Gouya *et al.* (36) evaluated the hemodynamic parameters of phase contrast MRI and demonstrated that azygos flow was a good predictor of HVPG ≥16 mmHg. Frankova *et al.* (37) found that LS assessed using two-dimensional shear-wave elastography was a reliable predictor of HVPG above 16 and 20 mmHg. In contrast to the SWE study, our results indicate that the measurement of LS is of little value for these two thresholds. We suspect that this discrepancy may be due to the varying liver disease etiology. Unfortunately, Frankova *et al.* (37) did not assess SS, which was proven to be a better predictor in our study. Notably, although our results indicated SS to have good diagnostic value overall, it should only be used to rule out elevated HVPG and high-risk EVs at the proposed thresholds. In addition, we found that fibrosis 4, an inexpensive and widely used indicator of liver fibrosis, may be a useful tool for HVPG prediction, and it even outperformed SS in detecting the presence or absence of HVPG ≥16 mmHg. If our results are corroborated by future studies, fibrosis 4 could potentially be used as an alternative to more advanced methods.

Although there are some technical concerns that may hinder the applicability of MRE, mainly the cost and the accessibility compared to ultrasound-based methods, MRE has several advantages, including enabling the viscoelastic assessment of whole organs and a higher technical success rate. Patients with CLD often require contrast-enhanced MRI examinations for liver cancer screening. Therefore, we believe that MRE can be integrated into a conventional liver MRI examination without increasing patient cost.

Our study has some limitations. First, the sample size was relatively small because, in addition to the limited number of HVPG measurements, the exclusion criteria of this study were quite restrictive. For example, we excluded patients with hepatic venous-to-venous communications, a condition that could lead to an underestimation of portal venous pressure by the HVPG value (38), which has been overlooked in most previous studies. We believe that the narrow selection of patients may yield stronger scientific data. Nevertheless, the performance of our criteria for SS by MRE in larger cohorts and other settings remains to be confirmed. The second limitation is that not all included patients underwent endoscopy; however, we do not believe this introduced bias, as the only reason for not performing endoscopy in some patients was that the time was too close to their last examination and was thus driven entirely by random chance. Third, in this study, we performed two-dimensional MRE scans and therefore assessed only the stiffness or elasticity characteristics of the organs. The introduction of three-dimensional MRE will allow us to fully assess the role of viscoelastic characteristics in a future study.

Conclusions

In this prospective study, we found that SS measured by two-dimensional MRE may be superior to LS and serum tests in revealing PH in patients with generally high HVPG values. However, when used alone, SS used with the recommended thresholds is more suitable for ruling out elevated HVPG and high-risk EVs.

Acknowledgments

We would like to express our enormous appreciation and gratitude to Fuliang He, Guanhua Zhang, Yuerong Li, and Chunyu Wang.

Funding: This work was supported by the National Key Research and Development Program of China (2021ZD0113205 to H.Y.), the National Natural Science Foundation of China (61871276 and 62171298 to Z.Y., 82071876 to D.Y.), the Beijing Municipal Administration of Hospitals' Youth Programme (QML20200108 to Z.Y.), and the Digestive Medical Coordinated Development Center of Beijing Hospitals Authority (XXT04 to Y.W.).

Footnote

Reporting Checklist: The authors have completed the STROBE reporting checklist. Available at https://qims.amegroups.com/article/view/10.21037/qims-22-1415/rc

Conflicts of Interest: All authors have completed the ICMJE

uniform disclosure form (available at https://qims.amegroups.com/article/view/10.21037/qims-22-1415/coif). The authors have no conflicts of interest to declare.

Ethical Statement: The authors are accountable for all aspects of the work in ensuring that questions related to the accuracy or integrity of any part of the work are appropriately investigated and resolved. The study was conducted in accordance with the Declaration of Helsinki (as revised in 2013) and was approved by the Institutional Review Board of Beijing Friendship Hospital (no. 2018-P2-142-01). Written consent forms were obtained from all patients.

References

1. Sanyal AJ, Bosch J, Blei A, Arroyo V. Portal hypertension and its complications. Gastroenterology 2008;134:1715-28.
2. Bosch J, Garcia-Pagán JC, Berzigotti A, Abraldes JG. Measurement of portal pressure and its role in the management of chronic liver disease. Semin Liver Dis 2006;26:348-62.
3. Bosch J, Abraldes JG, Berzigotti A, García-Pagan JC. The clinical use of HVPG measurements in chronic liver disease. Nat Rev Gastroenterol Hepatol 2009;6:573-82.
4. de Franchis R; Baveno V Faculty. Revising consensus in portal hypertension: report of the Baveno V consensus workshop on methodology of diagnosis and therapy in portal hypertension. J Hepatol 2010;53:762-8.
5. Qi X, Berzigotti A, Cardenas A, Sarin SK. Emerging non-invasive approaches for diagnosis and monitoring of portal hypertension. Lancet Gastroenterol Hepatol 2018;3:708-19.
6. Ronot M, Lambert S, Elkrief L, Doblas S, Rautou PE, Castera L, Vilgrain V, Sinkus R, Van Beers BE, Garteiser P. Assessment of portal hypertension and high-risk oesophageal varices with liver and spleen three-dimensional multifrequency MR elastography in liver cirrhosis. Eur Radiol 2014;24:1394-402.
7. Kennedy P, Stocker D, Carbonell G, Said D, Bane O, Hectors S, Abboud G, Cuevas J, Bolster BD Jr, Friedman SL, Lewis S, Schiano T, Bhattacharya D, Fischman A, Thung S, Taouli B. MR elastography outperforms shear wave elastography for the diagnosis of clinically significant portal hypertension. Eur Radiol 2022;32:8339-49.
8. Abe H, Midorikawa Y, Matsumoto N, Moriyama M, Shibutani K, Okada M, Udagawa S, Tsuji S, Takayama T. Prediction of esophageal varices by liver and spleen MR elastography. Eur Radiol 2019;29:6611-9.
9. Shin SU, Lee JM, Yu MH, Yoon JH, Han JK, Choi BI, Glaser KJ, Ehman RL. Prediction of esophageal varices in patients with cirrhosis: usefulness of three-dimensional MR elastography with echo-planar imaging technique. Radiology 2014;272:143-53.
10. Wagner M, Hectors S, Bane O, Gordic S, Kennedy P, Besa C, Schiano TD, Thung S, Fischman A, Taouli B. Noninvasive prediction of portal pressure with MR elastography and DCE-MRI of the liver and spleen: Preliminary results. J Magn Reson Imaging 2018;48:1091-103.
11. Shi Y, Qi YF, Lan GY, Wu Q, Ma B, Zhang XY, Ji RY, Ma YJ, Hong Y. Three-dimensional MR Elastography Depicts Liver Inflammation, Fibrosis, and Portal Hypertension in Chronic Hepatitis B or C. Radiology 2021;301:154-62.
12. Yoon H, Shin HJ, Kim MJ, Han SJ, Koh H, Kim S, Lee MJ. Predicting gastroesophageal varices through spleen magnetic resonance elastography in pediatric liver fibrosis. World J Gastroenterol 2019;25:367-77.
13. Morisaka H, Motosugi U, Ichikawa S, Sano K, Ichikawa T, Enomoto N. Association of splenic MR elastographic findings with gastroesophageal varices in patients with chronic liver disease. J Magn Reson Imaging 2015;41:117-24.
14. Gharib AM, Han MAT, Meissner EG, Kleiner DE, Zhao X, McLaughlin M, Matthews L, Rizvi B, Abd-Elmoniem KZ, Sinkus R, Levy E, Koh C, Myers RP, Subramanian GM, Kottilil S, Heller T, Kovacs JA, Morse CG. Magnetic Resonance Elastography Shear Wave Velocity Correlates with Liver Fibrosis and Hepatic Venous Pressure Gradient in Adults with Advanced Liver Disease. Biomed Res Int 2017;2017:2067479.
15. Danielsen KV, Hove JD, Nabilou P, Yin M, Chen J, Zhao M, Kallemose T, Teisner AS, Siebner HR, Ehman RL, Møller S, Bendtsen F. Using MR elastography to assess portal hypertension and response to beta-blockers in

patients with cirrhosis. Liver Int 2021;41:2149-58.
16. Berzigotti A, Rossi V, Tiani C, Pierpaoli L, Zappoli P, Riili A, Serra C, Andreone P, Morelli MC, Golfieri R, Rossi C, Magalotti D, Zoli M. Prognostic value of a single HVPG measurement and Doppler-ultrasound evaluation in patients with cirrhosis and portal hypertension. J Gastroenterol 2011;46:687-95.
17. Stanley AJ, Robinson I, Forrest EH, Jones AL, Hayes PC. Haemodynamic parameters predicting variceal haemorrhage and survival in alcoholic cirrhosis. QJM 1998;91:19-25.
18. Jepsen P, Ott P, Andersen PK, Sørensen HT, Vilstrup H. Clinical course of alcoholic liver cirrhosis: a Danish population-based cohort study. Hepatology 2010;51:1675-82.
19. Tajiri T, Yoshida H, Obara K, Onji M, Kage M, Kitano S, et al. General rules for recording endoscopic findings of esophagogastric varices (2nd edition). Dig Endosc 2010;22:1-9.
20. de Franchis R; Baveno VI Faculty. Expanding consensus in portal hypertension: Report of the Baveno VI Consensus Workshop: Stratifying risk and individualizing care for portal hypertension. J Hepatol 2015;63:743-52.
21. Yin M, Talwalkar JA, Glaser KJ, Manduca A, Grimm RC, Rossman PJ, Fidler JL, Ehman RL. Assessment of hepatic fibrosis with magnetic resonance elastography. Clin Gastroenterol Hepatol 2007;5:1207-1213.e2.
22. Silva AM, Grimm RC, Glaser KJ, Fu Y, Wu T, Ehman RL, Silva AC. Magnetic resonance elastography: evaluation of new inversion algorithm and quantitative analysis method. Abdom Imaging 2015;40:810-7.
23. Pugh RN, Murray-Lyon IM, Dawson JL, Pietroni MC, Williams R. Transection of the oesophagus for bleeding oesophageal varices. Br J Surg 1973;60:646-9.
24. Wiesner RH, McDiarmid SV, Kamath PS, Edwards EB, Malinchoc M, Kremers WK, Krom RA, Kim WR. MELD and PELD: application of survival models to liver allocation. Liver Transpl 2001;7:567-80.
25. Wang L, Feng Y, Ma X, Wang G, Wu H, Xie X, Zhang C, Zhu Q. Diagnostic efficacy of noninvasive liver fibrosis indexes in predicting portal hypertension in patients with cirrhosis. PLoS One 2017;12:e0182969.
26. DeLong ER, DeLong DM, Clarke-Pearson DL. Comparing the areas under two or more correlated receiver operating characteristic curves: a nonparametric approach. Biometrics 1988;44:837-45.
27. Procopet B, Berzigotti A, Abraldes JG, Turon F, Hernandez-Gea V, García-Pagán JC, Bosch J. Real-time shear-wave elastography: applicability, reliability and accuracy for clinically significant portal hypertension. J Hepatol 2015;62:1068-75.
28. Palaniyappan N, Cox E, Bradley C, Scott R, Austin A, O'Neill R, Ramjas G, Travis S, White H, Singh R, Thurley P, Guha IN, Francis S, Aithal GP. Non-invasive assessment of portal hypertension using quantitative magnetic resonance imaging. J Hepatol 2016;65:1131-9.
29. Vizzutti F, Arena U, Romanelli RG, Rega L, Foschi M, Colagrande S, Petrarca A, Moscarella S, Belli G, Zignego AL, Marra F, Laffi G, Pinzani M. Liver stiffness measurement predicts severe portal hypertension in patients with HCV-related cirrhosis. Hepatology 2007;45:1290-7.
30. Takuma Y, Nouso K, Morimoto Y, Tomokuni J, Sahara A, Toshikuni N, Takabatake H, Shimomura H, Doi A, Sakakibara I, Matsueda K, Yamamoto H. Measurement of spleen stiffness by acoustic radiation force impulse imaging identifies cirrhotic patients with esophageal varices. Gastroenterology 2013;144:92-101.e2.
31. Hirooka M, Ochi H, Koizumi Y, Kisaka Y, Abe M, Ikeda Y, Matsuura B, Hiasa Y, Onji M. Splenic elasticity measured with real-time tissue elastography is a marker of portal hypertension. Radiology 2011;261:960-8.
32. Lim JK, Groszmann RJ. Transient elastography for diagnosis of portal hypertension in liver cirrhosis: is there still a role for hepatic venous pressure gradient measurement? Hepatology 2007;45:1087-90.
33. Colecchia A, Montrone L, Scaioli E, Bacchi-Reggiani ML, Colli A, Casazza G, Schiumerini R, Turco L, Di Biase AR, Mazzella G, Marzi L, Arena U, Pinzani M, Festi D. Measurement of spleen stiffness to evaluate portal hypertension and the presence of esophageal varices in patients with HCV-related cirrhosis. Gastroenterology 2012;143:646-54.
34. Huwart L, Sempoux C, Vicaut E, Salameh N, Annet L, Danse E, Peeters F, ter Beek LC, Rahier J, Sinkus R, Horsmans Y, Van Beers BE. Magnetic resonance elastography for the noninvasive staging of liver fibrosis. Gastroenterology 2008;135:32-40.
35. Garcia-Tsao G, Friedman S, Iredale J, Pinzani M. Now there are many (stages) where before there was one: In search of a pathophysiological classification of cirrhosis. Hepatology 2010;51:1445-9.
36. Gouya H, Grabar S, Vignaux O, Saade A, Pol S, Legmann P, Sogni P. Portal hypertension in patients with cirrhosis: indirect assessment of hepatic venous pressure gradient by measuring azygos flow with 2D-cine phase-contrast

magnetic resonance imaging. Eur Radiol 2016;26:1981-90.
37. Frankova S, Lunova M, Gottfriedova H, Senkerikova R, Neroldova M, Kovac J, Kieslichova E, Lanska V, Urbanek P, Spicak J, Jirsa M, Sperl J. Liver stiffness measured by two-dimensional shear-wave elastography predicts hepatic vein pressure gradient at high values in liver transplant candidates with advanced liver cirrhosis. PLoS One 2021;16:e0244934.
38. de Franchis R, Bosch J, Garcia-Tsao G, Reiberger T, Ripoll C; Baveno VII Faculty. Baveno VII - Renewing consensus in portal hypertension. J Hepatol 2022;76:959-74.

Cite this article as: Han X, Yang D, Xu H, Wang Y, Yin H, Yang Z. Superiority of spleen stiffness on two-dimensional magnetic resonance elastography over liver stiffness and serum tests in assessing portal hypertension in chronic liver disease. Quant Imaging Med Surg 2024;14(2):1429-1440. doi: 10.21037/qims-22-1415

Supplementary

Table S1 Univariable and multivariable logistic regression analysis of parameters for patients with HVPG ≥16 mmHg

Variable	Univariable			Multivariable		
	Odds ratio	95% CI	P	Odds ratio	95% CI	P
Age	1.039	0.989–1.092	0.13			
Male sex	0.625	0.198–1.974	0.42			
BMI	1.038	0.906–1.188	0.59			
Albumin	0.935	0.861–1.016	0.11			
Total bilirubin	1.016	0.995–1.038	0.13			
Serum creatinine	0.975	0.939–1.012	0.18			
AST	1.001	0.996–1.007	0.67			
ALT	0.997	0.991–1.003	0.36			
Platelet count	0.978	0.961–0.995	0.01			
Prothrombin time	0.941	0.627–1.410	0.77			
INR	13.118	0.716–240.506	0.08			
MRE-LS	1.209	0.925–1.580	0.17			
MRE-SS	1.614	1.202–2.166	0.001	1.614	1.202–2.166	0.001
Child-Pugh score	1.516	1.072–2.142	0.02			
MELD score	1.049	0.923–1.192	0.46			
Fibrosis 4	1.314	1.096–1.577	0.003			
APRI	1.112	0.958–1.290	0.16			
King's score	1.004	0.998–1.010	0.15			

Bolded type indicates variables included in the multivariable analysis. HVPG, hepatic venous pressure gradient; CI, confidence interval; BMI, body mass index; AST, aspartate transaminase; ALT, alanine transaminase; INR, international normalized ratio; MRE-LS, magnetic resonance elastography–liver stiffness; MRE-SS, magnetic resonance elastography–spleen stiffness; MELD, model for end-stage liver disease; APRI, aspartate aminotransferase-to-platelet ratio index.

Table S2 Univariable and multivariable logistic regression analysis of parameters for patients with HVPG ≥20 mmHg

Variable	Univariable			Multivariable		
	Odds ratio	95% CI	P	Odds ratio	95% CI	P
Age	1.053	0.994–1.117	0.08	1.108	1.010–1.216	0.03
Male sex	0.727	0.222–2.387	0.60			
BMI	1.003	0.874–1.151	0.96			
Albumin	0.934	0.852–1.025	0.15			
Total bilirubin	0.999	0.988–1.009	0.79			
Serum creatinine	0.985	0.948–1.023	0.43			
AST	1.002	0.997–1.007	0.51			
ALT	0.997	0.991–1.004	0.41			
Platelet count	0.980	0.962–0.998	0.03			
Prothrombin time	0.768	0.470–1.254	0.29			
INR	14.318	0.836–245.294	0.07	206.962	2.309–18,547.320	0.02
MRE-LS	1.107	0.854–1.435	0.44			
MRE-SS	1.685	1.232–2.304	0.001	2.096	1.318–3.333	0.002
Child-Pugh score	1.390	1.005–1.923	0.05			
MELD score	1.005	0.883–1.145	0.94			
Fibrosis 4	1.142	1.030–1.266	0.01			
APRI	1.097	0.968–1.242	0.15			
King's score	1.004	0.999–1.009	0.10			

Bolded type indicates variables included in the multivariable analysis. HVPG, hepatic venous pressure gradient; CI, confidence interval; BMI, body mass index; AST, aspartate transaminase; ALT, alanine transaminase; INR, international normalized ratio; MRE-LS, magnetic resonance elastography–liver stiffness; MRE-SS, magnetic resonance elastography–spleen stiffness; MELD, model for end-stage liver disease; APRI, aspartate aminotransferase-to-platelet ratio index.

https://dx.doi.org/10.21037/qims-22-1415

Table S3 Univariable and multivariable logistic regression analysis of parameters for patients with high-risk EVs

Variable	Univariable			Multivariable		
	Odds ratio	95% CI	P	Odds ratio	95% CI	P
Age	1.026	0.964–1.091	0.42			
Male sex	0.656	0.173–2.488	0.54			
BMI	0.965	0.819–1.137	0.67			
Albumin	0.894	0.797–1.004	0.06			
Total bilirubin	0.964	0.934–0.995	0.02			
Serum creatinine	0.977	0.933–1.022	0.31			
AST	0.993	0.984–1.002	0.14			
ALT	0.991	0.981–1.001	0.09			
Platelet count	0.972	0.951–0.993	0.01			
Prothrombin time	0.798	0.473–1.348	0.40			
INR	0.241	0.006–10.266	0.46			
MRE-LS	0.814	0.603–1.097	0.18			
MRE-SS	2.076	1.282–3.362	0.003	2.076	1.282–3.362	0.003
Child-Pugh score	0.977	0.718–1.332	0.89			
MELD score	0.831	0.697–0.991	0.04			
Fibrosis 4	1.019	0.912–1.139	0.74			
APRI	0.913	0.774–1.077	0.28			
King's score	0.997	0.991–1.002	0.26			

Bolded type indicates variables included in the multivariable analysis. EVs, esophageal varices; CI, confidence interval; BMI, body mass index; AST, aspartate transaminase; ALT, alanine transaminase; INR, international normalized ratio; MRE-LS, magnetic resonance elastography–liver stiffness; MRE-SS, magnetic resonance elastography–spleen stiffness; MELD, model for end-stage liver disease; APRI, aspartate aminotransferase-to-platelet ratio index.

Table S4 Difference in the AUC between noninvasive markers in the diagnosis of HVPG ≥16 mmHg

	MRE-SS	albumin	PLT count	Child-Pugh score	Fibrosis 4	APRI
Albumin	0.095, 0.36					
PLT count	0.019, 0.77	0.076, 0.46				
Child-Pugh score	0.082, 0.43	0.013, 0.46	0.063, 0.52			
Fibrosis 4	0.054, 0.53	0.149, 0.08	0.073, 0.30	0.136, 0.08		
APRI	0.046, 0.66	0.050, 0.58	0.026, 0.76	0.037, 0.61	0.100, 0.09	
King's score	0.007, 0.95	0.102, 0.23	0.026, 0.77	0.089, 0.17	0.047, 0.32	0.052, 0.11

Data are expressed as the difference between areas, P value. Differences in the AUC between two markers were determined using the DeLong test. AUC, area under the curve; HVPG, hepatic venous pressure gradient; MRE-SS, magnetic resonance elastography–spleen stiffness; PLT, platelet; APRI, aspartate aminotransferase-to-platelet ratio index.

https://dx.doi.org/10.21037/qims-22-1415

Table S5 Difference in the AUC between noninvasive markers for the diagnosis of HVPG ≥20 mmHg

	MRE-SS	Albumin	PLT count	Fibrosis 4	APRI
Albumin	0.115, 0.28				
PLT count	0.082, 0.34	0.033, 0.77			
Fibrosis 4	0.044, 0.66	0.070, 0.50	0.037, 0.53		
APRI	0.137, 0.21	0.022, 0.82	0.056, 0.47	0.093, 0.08	
King's score	0.080, 0.46	0.035, 0.72	0.002, 0.98	0.035, 0.36	0.057, 0.08

Data are expressed as the difference between areas, P value. Differences in AUC between two markers were determined using the DeLong test. AUC, area under the curve; HVPG, hepatic venous pressure gradient; MRE-SS, magnetic resonance elastography–spleen stiffness; PLT, platelet; APRI, aspartate aminotransferase-to-platelet ratio index.

Table S6 Difference in the AUC between noninvasive markers for the diagnosis of high-risk EVs

	MRE-SS	Albumin	PLT count	Total bilirubin
Albumin	0.181, 0.15			
PLT count	0.083, 0.36	0.098, 0.42		
Total bilirubin	0.143, 0.23	0.038, 0.81	0.060, 0.66	
MELD score		0.016, 0.92	0.083, 0.54	0.022, 0.74

Data are expressed as the difference between areas, P value. Differences in the AUC between the two markers were determined using the DeLong test. AUC, area under the curve; EVs, esophageal varices; MRE-SS, magnetic resonance elastography–spleen stiffness; PLT, platelet; MELD, model for end stage liver disease.

https://dx.doi.org/10.21037/qims-22-1415